Article

The Use of Multi-Temporal Landsat Imageries in Detecting Seasonal Crop Abandonment

Noryusdiana Mohamad Yusoff [1,2] and Farrah Melissa Muharam [1,3,*]

[1] Department of Agriculture Technology, Faculty of Agriculture, University Putra Malaysia, UPM Serdang, Selangor 43400, Malaysia

[2] Malaysian Remote Sensing Agency, No. 13, Jalan Tun Ismail, Kuala Lumpur 50480, Malaysia; E-Mail: noryusdiana@remotesensing.gov.my

[3] Institute of Plantation Studies, University Putra Malaysia, UPM Serdang, Selangor 43400, Malaysia

* Author to whom correspondence should be addressed; E-Mail: farrahm@upm.edu.my; Tel.: +60-3-8947-4960; Fax: +60-3-8938-1015.

Abstract: Abandonment of agricultural land is a global issue and a waste of resources and brings a negative impact on the local economy. It is also one of the key contributing factors in certain environmental problems, such as soil erosion and carbon sequestration. In order to address such problems related to land abandonment, their spatial distribution must first be precisely identified. Hence, this study proposes the use of multi-temporal Landsat imageries, together with crop phenology information and an object-oriented classification technique, to identify abandoned paddy and rubber areas. Results indicate that Landsat time-series images were highly beneficial and, in fact, essential in identifying abandoned paddy and rubber areas, particularly due to the unique phenology of these seasonal crops. To differentiate between abandoned and non-abandoned paddy areas, a minimum of three time-series images, mainly acquired during the planting seasons is required. For rubber, multi-temporal images should be examined in order to confirm the wintering season. The study demonstrates the advantages of using multi-temporal Landsat imageries in identifying abandoned paddy and rubber areas wherein an accuracy of 93.33% ± 14% and 83.33% ± 1%, respectively, were achieved.

Keywords: multi-temporal satellite imagery; seasonal crop; land abandonment; remote sensing

1. Introduction

Detecting land abandonment has become one the most important global agenda and political discussions in recent decades due to the strong relationship that the environment has with the socio-economy of a country [1,2]. Land abandonment has also been identified as one of the key contributing factors of soil erosion [3] and increasing carbon sequestration [4–6], as well as having implications on landscape planning [2]. From the economic point of view, abandonment of agricultural land means that resources are wasted and food production is decreased, thus negatively affecting the local economy [7].

Land abandonment is commonly associated with the land cover changing from an agriculture land to an arboreous shrubland or a secondary forest [2]. Additionally, it is identified as a heterogeneous area [4,8,9] or an area with high variability in terms of reflectance [7]. In the Malaysian context, agricultural land is considered abandoned when the area has a minimum coverage of at least 0.4 hectares and is left uncultivated for three consecutive years or more [10]. In 2014, a total area of 119,273 hectares, or 2%, of Peninsular Malaysia's arable soil was declared abandoned [10]. This statistic however, can dynamically fluctuate due to any additions of newly abandoned lands or the development of previously abandoned lands [10]. According to Ponnusamy [11], abandoned lands are commonly scattered and widespread [4]; hence, to detect and identify them can pose quite a challenge in terms of cost, time, and labor.

Advanced technology, such as remote sensing, has been useful in identifying abandoned lands [1]. By employing remote sensing imagery, complemented by an object-oriented classification technique, an automatic procedure of monitoring abandoned lands [7] with fast results can be performed. While studies on detection of abandoned agricultural land in Malaysia are almost nil, such studies have been carried out in other countries [1,4,9,12] where satellite imageries such as Landsat TM, MODIS, and IKONOS were utilized. These studies show that remote sensing is greatly useful in studying land abandonment, especially when large areas are involved, since the images could provide reliable land-use data from previous years. Nevertheless, most of these studies looked at annual crops rather than perennial crops, as they dominate many equatorial countries.

In utilizing remote sensing imagery to detect abandoned lands, multi-temporal images can also be used as a strategy [13] in achieving the best possible classification accuracy [14] and in estimating vegetation phenology [15]. This is because the changes in the reflectance during the cropland cycle are recorded by satellites and, thus, can be observed with multi-temporal images [1]. While the dates of these images are undeniably important, it is also essential to note that the key dates differ between abandoned classes [1]. For annual crops, for instance, ideally three images should be captured during spring, summer, and fall of a single year for both pre- and post-abandonment periods. On the other hand, the usage of satellite images from many dates is preferable for accurate monitoring of non-annual crops [1]. Moreover, for crops such as rubber, its unique phenological characteristic is shown during foliation and defoliation stages [16], or growing and non-growing seasons, where during the growing seasons, its NDVI value is high and similar to an evergreen forest [17]. As for paddy, its unique phonological characteristic is shown during the flooding and transplanting phase [18].

Nowadays, the object-oriented classification methodology is also becoming more popular than the traditional pixel-based technique, which has been studied by many researchers [19–23]. With the object-oriented technique, the rule set protocol can be developed and transferred between images in a

multi-temporal analysis, provided that image normalization has been performed [22]. This method also performs better than pixel-based classification techniques, especially in reducing spectral variability [20]. Milenov *et al.* [7] also found that the object-oriented method can produce an acceptable level of accuracy in monitoring the risk of farmland abandonment. Furthermore, this technique offers the possibility of integrating satellite imagery with other existing vector data during the process of object identification [24,25].

This paper aims to utilize the multi-temporal images of Landsat TM/OLI in identifying paddy and rubber land abandonment in Malaysia. These crops contribute vitally to the country's gross domestic product (GDP), which is USD 1.6 billion and USD 0.4 billion, annually, for rubber and paddy, respectively. Assessing the status of paddy land abandonment is crucial not only because it is widely planted after oil palm and rubber, but also due to the fact that the local production of paddy is only at 70%, leaving the country dependent on the importation of rice. Hence, having an abandonment monitoring program for this crop will help the country's long term food security program. Therefore, in order to meet the objective of this research, that is, to develop a rule-based classification methodology in identifying abandoned rubber and paddy areas using multi-temporal Landsat images, the following research questions need to be answered:

1. What is the total area of abandoned paddy and rubber in the study area?
2. How accurately can abandoned paddy and rubber areas be identified using rule-based classification with multi-temporal Landsat imageries?

2. Methods

2.1. Study Area

This study was conducted in Mukim of Sungai Siput and Kuala Kangsar, Perak (Figure 1), covering an area of approximately 96,816 hectares. Its exact location is from 5°5′51″N, 100°48′59″E to 4°39′12″N, 101°28′2″E. The study area has a tropical climate with temperatures ranging from 24 °C to 33 °C. Humidity level is generally 86% and daily rainfall is 6 mm. The soil types in this area are predominantly sandy clay, sandy clay loam, sandy loam, sandy, and silty clay. The topography in this area is relatively hilly from 18 to 1790 m where almost 50% of this area is covered by primary forest.

2.2. Data Collection

In this study, multi-temporal imageries of a 30-m resolution Landsat TM/OLI satellite were utilized. A systematic archiving of data gathered was obtained from the United States Geological Survey (USGS). Fifteen series of Landsat images were acquired (Table 1). Images dating from 2013 onwards were used to develop the phenological characteristics of rubber and paddy, while images dated as 2014 were purposely used for image classification and feature extraction, corresponding with the ground data collection dates. The historical images from 1997 and 2009 were used for image normalization and for supporting the feature extraction of abandoned land.
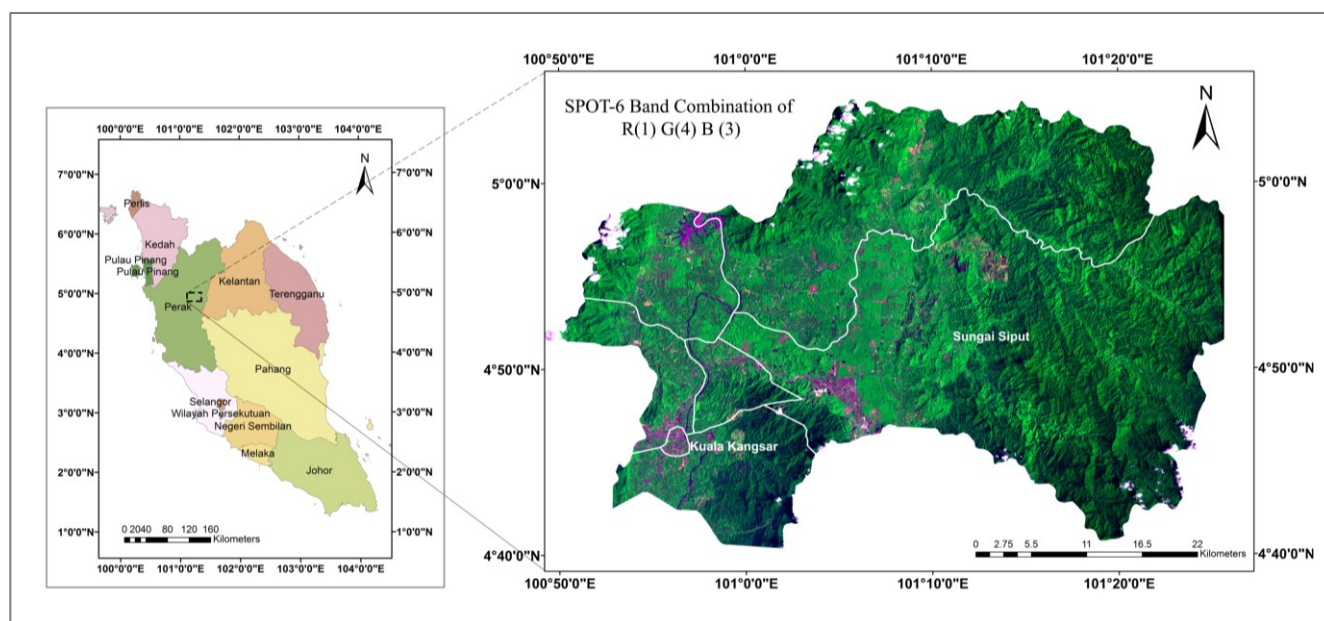
Figure 1. Study area in Mukim of Sungai Siput and Kuala Kangsar, Perak, Malaysia.

Table 1. Landsat images acquisition.

Image Date	Sensor	Image Purpose
28 May 1997	TM	Reference for image normalization
21 January 2009	TM	Supporting the feature extraction of abandoned land
22 April 2013	OLI	Crop phenology development
9 June 2013	OLI	Crop phenology development
18 December 2013	OLI	Crop phenology development
4 February 2014	OLI	Crop phenology development and classification
24 March 2014	OLI	Crop phenology development
9 April 2014	OLI	Crop phenology development
11 May 2014	OLI	Crop phenology development
28 June 2014	OLI	Crop phenology development and classification
16 September 2014	OLI	Crop phenology development and classification
7 February 2015	OLI	Crop phenology development
23 February 2015	OLI	Crop phenology development
11 March 2015	OLI	Crop phenology development
12 April 2015	OLI	Crop phenology development

For classification and feature extraction, a historical land use map prepared in 2006 acquired from [10] was also used, providing an 8-year gap between the ancillary data and satellite imagery used for classification. A longer gap is chosen in order to meet the definition of abandoned land [10], that is, land abandoned for at least three years and also to avoid the problem of misidentifying poorly managed or unmanaged plantation as an abandoned land, as it could physically resemble one.

Ground locations of abandoned agricultural paddy and rubber were obtained for phenology development and accuracy assessment. Field trips were then conducted throughout the entire study area on January, April, and November 2014. Additionally, an image from SPOT-6 with a 1.5 m resolution dated as 12 February 2014 was used to complement the classification accuracy assessment. A total of

120 locations were found, with 30 locations each for abandoned and non-abandoned paddy, and also for abandoned and non-abandoned rubber.

Crop seasonal information, such as rubber wintering season and paddy planting dates, were also obtained in order to verify the crop phenology derived from the time-series images. For rubber, two (2) seasons are involved: primary (July to September) and secondary (February to March) [26]. For paddy, the first season is often at the beginning of February and the second season usually begins in June or July [27].

2.3. Crop Phenology Development

Crop phenology for paddy and rubber was developed using the vegetation indices extracted from the Landsat time-series images from 2013 to 2015. Vegetation indices which are mostly derived from the combination of two spectral bands were used in order to minimize the effect of external factors on the spectral data [28]. Normalized Difference Vegetation Index (NDVI), sensitive to the greenness of vegetation [29] and the most commonly used vegetation index in various vegetation studies [28,30–32], was used. The NDVI values of each abandoned and non-abandoned crops from the 2013 images were extracted based on the coordinates of these locations on the ground. The average NDVI value was then calculated for each satellite image. Finally, the crop phenology graph was created in order to understand the characteristics of satellite images that should be selected for the classification analysis.

2.4. Pre-Processing of Satellite Images

2.4.1. Digital Number (DN) to Reflectance Conversion

When comparing images from different sensors and platforms, the conversion of image data from DN to spectral radiance to Top-Of-Atmosphere (TOA) reflectance is a common and fundamental step. For this, the standard equation provided by USGS [33] for Landsat OLI and Chander *et al.* [34] for Landsat TM was utilized. The general processing workflow is shown in Figure 2.

2.4.2. Image Normalization

Since multi-temporal satellite images were used, image normalization is critical and necessary in order to ensure the homogeneity of the Landsat time-series data set. This is achieved by adjusting the radiometric properties of an image series based on a single reference image [35]. In this study, normalization is performed using the histogram matching method by Pratt [36]. An image dated as 28 May 1997 was chosen as the reference image and the histogram of this reference image was matched to the rest of the images.

2.5. Image Classification and Feature Extraction

The object-oriented approach was adopted as the classification method in this research. Feature extraction combines the process of segmenting an image into regions of pixels, computing attributes for each region to create objects, and classifying the objects based on attributes to extract features. Landsat OLI images with dates as illustrated in Table 2 were used as image inputs with R(6)

G(5) B(4) band combinations as recommended for vegetation analysis [37]. NDVI images and rasterized land use maps were also integrated as ancillary data input.

Table 2. The rule set protocol to classify abandoned and non-abandoned paddy and rubber.

	Paddy	**Rubber**
Primary Image Input	4 February 2014 28 June 2014 16 September 2014	4 February 2014
Ancillary Data Input	NDVI Land use 2006 (Rasterized)	Land use 2006 (Rasterized)
Scale Parameter	20	20
Merge Level	60	60
Rule Set	**Land preparation phase** Land use (Confidence image value) < 210 NDVI < 0.3521 SWIR 1 (Reflectance) > 0.1746	**Non-abandoned** Land use (Confidence image value) < 250 NIR (Reflectance) < 0.4760
	Pre-Planting (Irrigation phase) Land use (Confidence image value) < 210 NDVI < 0.3521 SWIR 1 (Reflectance) NOT > 0.1746 SWIR 2 (Reflectance) < 0.0544	**Abandoned** Land use (Confidence image value) < 250 NIR (Reflectance) NOT < 0.4760
	Crop growth phase Land use (Confidence image value) < 210 SWIR 1 (Reflectance) NOT > 0.1746 SWIR 2 (Reflectance) NOT < 0.0544	

For image segmentation, the scale selected will directly affect the classification accuracy. The scale of segmentation should be proportionate to the image resolution [38]. Thus, in order to obtain the optimal segmentation scale, the segmentation was executed under three different scale levels of 10, 20, and 30. The result showed that the best scale level is 20 since the images of objects created at the scale level of 10 were too small while at the scale level of 30, the objects created were too large. Hence, this data file was created using a scale level of 20 and a merge level of 60. The same segmentation parameters were kept in mind while importing other images since the similar rule set needs to be applied to other satellite images.

In the development of the rule set, the thresholds were identified by adjusting the range given by the image histogram based on the researchers' visual analysis [39]. To ensure that the range is correct, a preview result window was used for visual interpretation. Therefore, this technique requires the user to have knowledge of the study area or the fundamental characteristic of the object features [40], similar to supervised classification, except that no training area is needed.

For object identification of non-abandoned and abandoned paddy areas, three OLI images dated as 4 February, 28 June, and 16 September 2014 were selected based on the paddy phenology information obtained from the multi-temporal Landsat images. In these time-series images displayed in band combinations of R(6), G(5), B(4), paddy cultivation areas could appear in any of these three colors: red, blue, or green, due to different planting activities. Red-colored paddy areas were associated with land preparation phase, where the areas were mostly covered with soil. Blue-colored paddy areas reflected

pre-planting phase involving irrigation phase, known as "flood/open-canopy phase" where the paddy rice fields are a mixture of water and paddy plants [18]. While the paddy is growing, the optical sensor only measures the plants, thus appearing in green [18].

For delineating the paddy areas, the vector land use map of paddy areas was first rasterized based on the land use code. After the importation and segmentation processes, the rasterized land use map was displayed in an 8-bit image called a confidence image, with values ranging from 0 to 255. Then the threshold of the confidence image was set to less than 210, representing the paddy area boundary. The accuracy of the generated boundary was then examined by overlaying it on the original vector land use map.

For the land preparation and irrigation phases, NDVI values less than 0.3521 were chosen, representing non-vegetated area. Then to complement the NDVI band, the SWIR band which is sensitive to both leaf area and leaf water content was used [29]. The value of the SWIR 1 band was specified to more than 0.1746 for the land preparation phase, representing the reflection from the mixture of soil and paddy plant. Since the soil tends be dry in the early planting stage, less absorption occurs at this wavelength, resulting in an increase in their threshold values. For the irrigation phase, the values of SWIR 1 band were assigned to not more than 0.1746. Since the paddy patches were mainly a reflection of a mixture of water and paddy plant, more water absorption was expected at this wavelength. In order to strengthen these rule sets, the value of SWIR 2 band was also specified to be less than 0.0544 for the irrigation phase. As for the crop growth phase, different threshold values were defined, where SWIR 1 band was set to not more than 0.1746 and SWIR 2 band was set to not less than 0.0544.

Finally, we employed the same rule set to the other images dated as 28 June and 16 September 2014 in order to examine any possible planting activities conducted throughout the year. The hypothesis is, if the paddy areas permanently appear evergreen in these two images, there is a high possibility that the areas are abandoned. This is also confirmed by Dong *et al.* [18] who stated that "evergreen vegetation has green leaves all year round, with no period of defoliation".

In identifying and distinguishing between abandoned and non-abandoned rubber areas, crop phenology information obtained from the multi-temporal satellite images was also used. The unique characteristic for rubber plantation is the defoliation (leaf-off) and foliation (new leaf emergence) phases [16]. Based on the aforementioned knowledge, an image dated as 4 February 2014 was selected. In this image displayed in band combinations of R(6), G(5), B(4), the non-abandoned areas appeared in brown-green color due to the unique defoliation phenology, while abandoned areas were light-green in color. At the defoliation stage, the rubber canopy is either covered with little or no green leaves, resulting in low NDVI values [16]. NIR band was utilized since the reflectance increases nonlinearly with the number of leaf layers, where a full canopy reflects 85% more light than a single leaf layer [29]. To delineate the rubber areas, the threshold range for the rasterized land use image was set to less than 250. Consequently, to complement the rule set development, the NIR value was set to less than 0.4760 in order to delineate the non-abandoned rubber from the abandoned rubber areas.
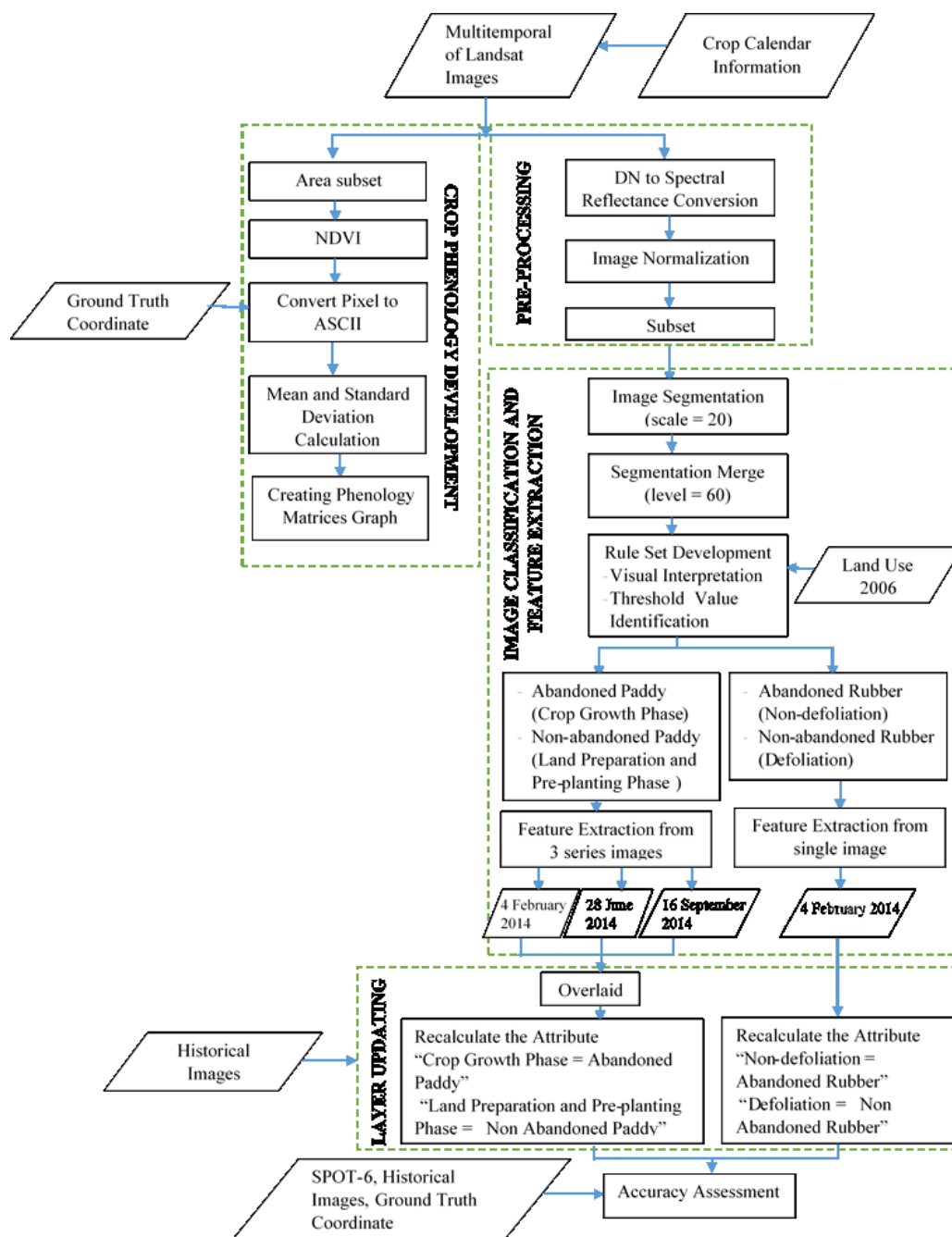
Figure 2. Workflow for abandoned and non-abandoned paddy and rubber feature extraction.

2.6. Layer Updating

To finalize the findings, the classification results were overlaid with the historical Landsat TM image dated as 21 January 2009, providing a five-year gap in order to confirm any abandonment status. Paddy areas that depicted land preparation and irrigation activities were renamed as non-abandoned paddy while paddy areas that consistently appeared to be in a crop growth phase were labeled as abandoned paddy. Meanwhile, the defoliated rubber areas were renamed as non-abandoned rubber, and the non-defoliated rubber areas as abandoned rubber. The final classification procedure involved eliminating any areas less than 0.4 hectares in order to meet the definition of an abandoned agricultural land [10].

2.7. Accuracy Assessment

For the accuracy assessment, all of the ground data points, the SPOT-6 image, and the historical Landsat images were utilized. Thirty sample points for each of the four classes (abandoned paddy, non-abandoned paddy, abandoned rubber, and non-abandoned rubber) were located using stratified random sampling, where the number of points is stratified to the distribution of the classification classes [41]. In total, 120 independent points were used for the purpose of validation. According to Dong *et al.* [18], the land cover classification accuracy is influenced by three factors: (i) quality of satellite image, (ii) *in situ* data, and (iii) algorithm. Standard error, $S(\hat{p})$ and standard error of adjusted area, $S(\hat{A})$, which incorporate user and producer accuracy with known area proportions of the map classes, Wi, were then calculated for each class [42].

3. Results and Discussion

3.1. Crop Phenology

3.1.1. Paddy

As seen in Figure 3 below, the NDVI values for abandoned and non-abandoned paddy areas are clearly distinct. For the non-abandoned paddy area, the NDVI values recorded were low for the 4 February 2014 and 7 February 2015 images, while high values were recorded for the 9 June 2013 and 11 May 2014 images. The low NDVI could be attributed to activities where paddy crops were absent, such as seedling or irrigation, while the high values could indicate the presence of paddy crops such as during the growth phase. The phenology for the abandoned paddy area meanwhile is evidently different from the non-abandoned paddy, where the NDVI values were consistently high throughout the time-series images [18]. These areas were found to be covered by grasses and bushes (Figure 3ii) with no presence of paddy planting activities such as land preparation and pre-planting.
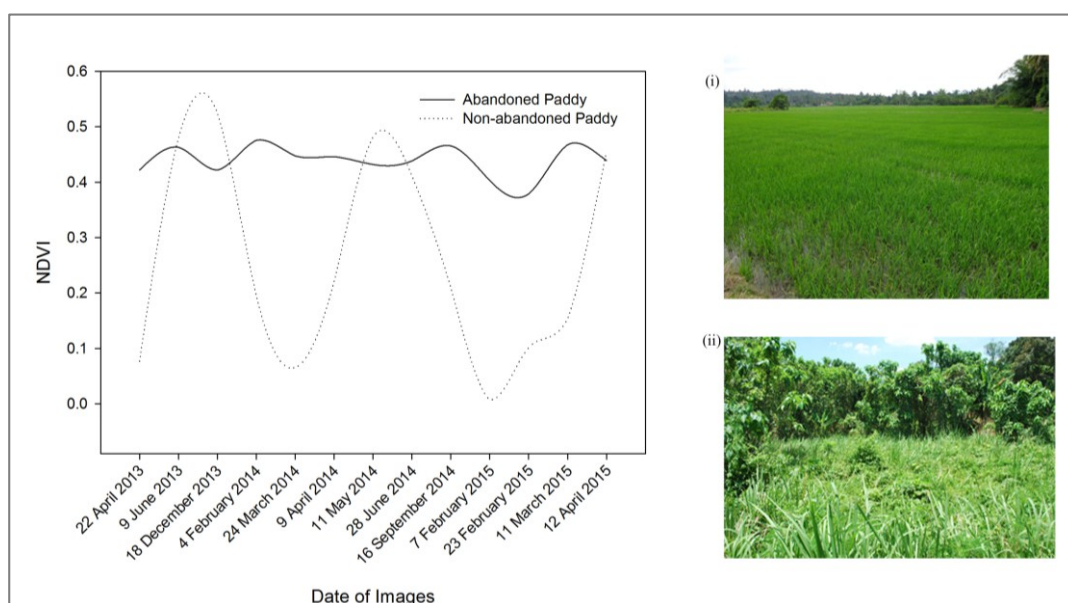

Figure 3. Phenology for paddy; (**i**) non-abandoned paddy; (**ii**) abandoned paddy.

To demonstrate the importance of time-series images in discriminating between abandoned and non-abandoned paddy areas, images of three paddy cultivation areas with three different dates (4 February, 28 June, and 16 September 2014) were also selected (Figure 4). Changes in color, either to red or blue, can be clearly seen in the images of the first (area I) and third (area III) paddy cultivation areas during the period where different paddy planting activities were carried out (Figure 4a–c,g–i). The second paddy cultivation area (area II) (Figure 4d–f) however, maintained its green color throughout the selected period despite the fact that these images were obtained during the planting season.
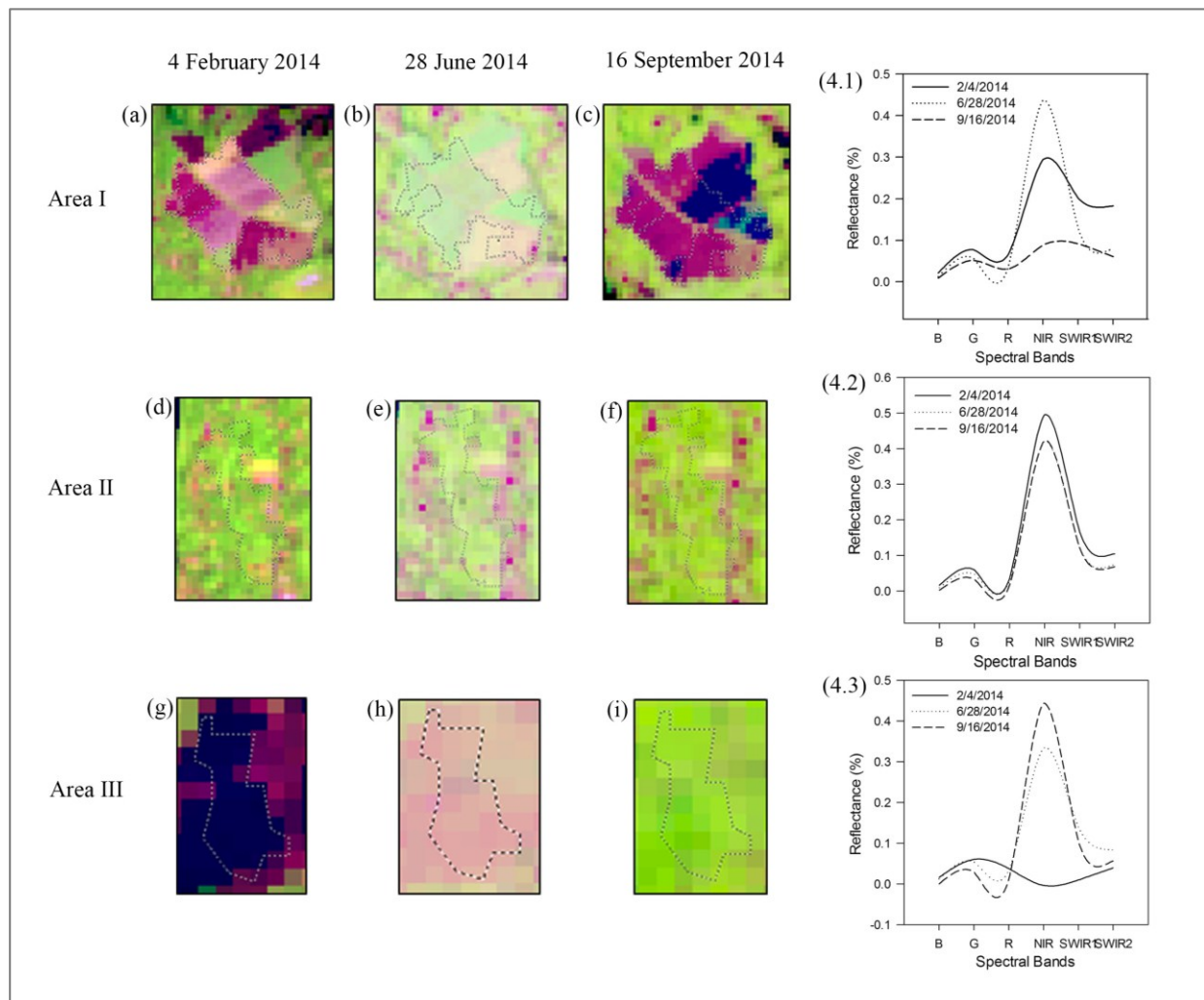

Figure 4. Landsat time-series imagery for three selected paddy areas (**a–i**); (**4.1**) spectral reflectance for area I; (**4.2**) spectral reflectance for area II; and (**4.3**) spectral reflectance for area III.

In terms of spectral reflectance of paddy cultivation areas, Figures 4.1 and 4.3 demonstrate the reflectance of different types of features while Figure 4.2 only shows the spectral signature of vegetation. Low reflectance is observed for both areas I and III in the 16 September 2014 image and 4 February 2014 image, respectively. The shape of the spectral signature resembles that of water bodies, where these images were possibly acquired during the irrigation phase. For area I and III, two types of energy could be identified from the unique spectral signature of vegetation: (i) low energy in the NIR wavelength, which could be attributed to young vegetation, where in the early stages, paddy crops are

mixed with background soil; and (ii) high energy in the NIR region due to the grown paddy crops where they dominate the background soil. Since the reflectance indicates planting activities, these areas were identified as non-abandoned. As for the spectral reflectance in Figure 4.2, it remained unchanged in the three images, suggesting that these are permanently vegetated areas, such as with shrubs or bushes, or abandoned areas. From this, it is important to note that if images from only a single date were used instead, such as the ones dated as 28 June 2014, misclassification could possibly occur due to the similar NDVI readings for both abandoned and non-abandoned paddy areas as all represent vegetated areas. If images from another date possessing lower NDVI values were used, other classes such as soil or water body could be represented. Therefore, the utilization of multi-temporal satellite images based on the planting activities is crucial to discriminate between abandoned and non-abandoned paddy areas.

3.1.2. Rubber

Figure 5 below shows the NDVI values for abandoned and non-abandoned rubber areas using multi-temporal Landsat images. The differences in the NDVI values between abandoned and non-abandoned rubber were not too evident, except for the lower and higher NDVI values for non-abandoned rubber for the 4 February and 9 April 2014 images. It was hypothesized that the lower NDVI value was due to the higher mean temperatures in February 2015 [43], causing noticeable defoliation in the non-abandoned rubber plantation, as dry monsoon is known to contribute to defoliation [16]. On the other hand, the NDVI value for the abandoned rubber was high due to the heterogeneous condition of the abandoned areas where evergreen crops were not subjected to defoliation. While the month of February is known as the defoliation season for rubber, images dated as 7 and 23 February 2015 did not depict this vital crop phenology information.
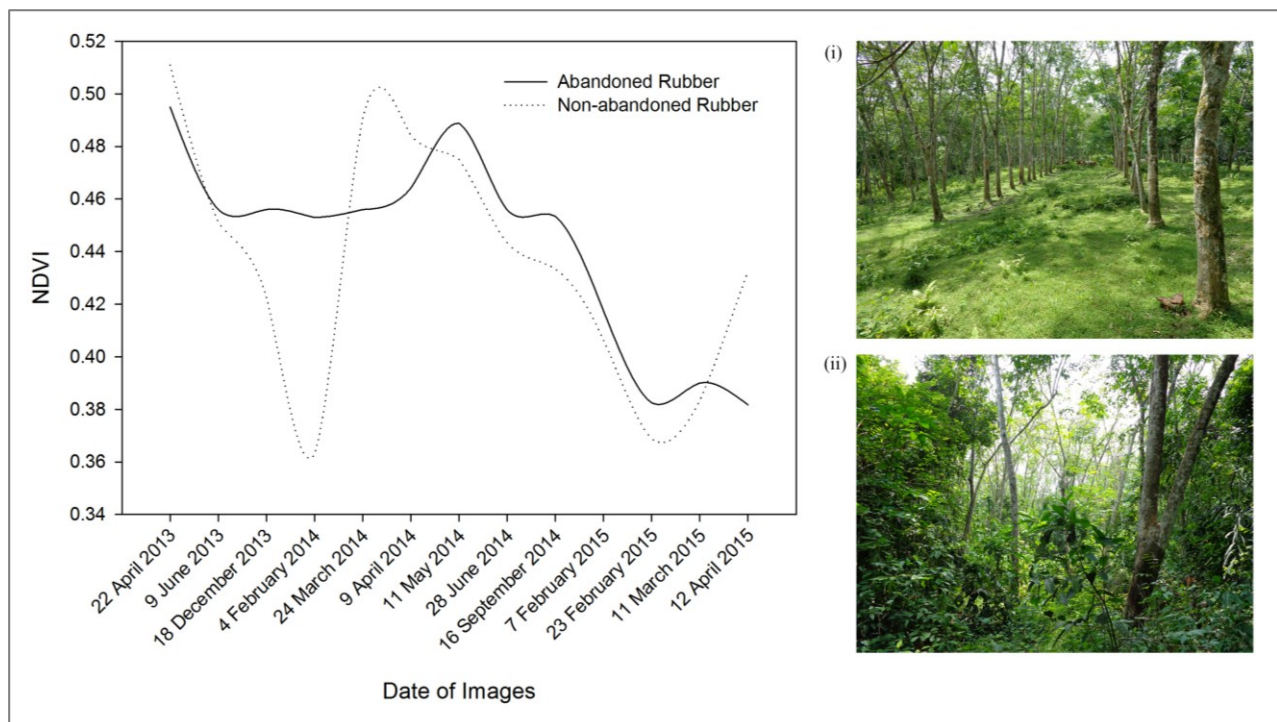

Figure 5. Phenology for rubber; (**i**) non-abandoned rubber; (**ii**) abandoned rubber.

In discriminating between abandoned and non-abandoned rubber areas, information on the wintering season is essential in order to select the right satellite images based on the appropriate phenology phases. The implications of ignoring this information on wintering will not only result in the difficulty to differentiate the abandoned areas, but will also pose a major challenge in discriminating between rubber and oil palm via visual interpretation and unsupervised classification, as demonstrated in Figure 6a–c. For instance, if the classification procedure is implemented on images dated as 28 June or 16 September 2014, rubber and oil palm classes would be indistinguishable as demonstrated by mark points I, II, and III in Figure 6b,c.
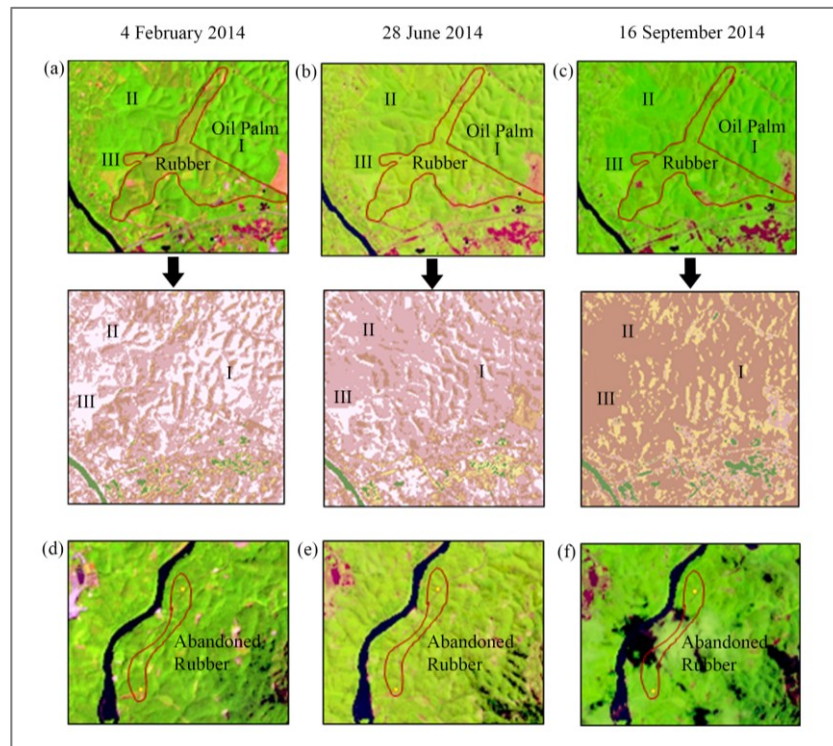

Figure 6. Multi-temporal Landsat OLI imagery used to choose the right satellite image in discriminate between non-abandoned rubber and oil palm; (**a**) images dated as 4 February 2014; (**b**) images dated as 28 June 2014; (**c**) images dated as 16 September 2014; and abandoned rubber appear permanently green using time series image (**d**) images dated as 4 February 2014; (**e**) images dated as 28 June 2014; (**f**) images dated as 16 September 2014.

From the visual interpretation, it can be seen that non-abandoned rubber areas appear in brown-green color during the wintering season, or defoliation stage, while abandoned rubber areas are permanently in green, mainly due to the mixed presence of rubber and other non-defoliating woody trees (Figure 6d–f).

3.2. Image Classification and Accuracy Assessment

3.2.1. Paddy

The final results for paddy classification were extracted from the combination of 2014 Landsat OLI time-series images and the 2009 historical Landsat TM image (Figure 7). Ground visits confirmed that

the abandoned paddy areas were vegetated by grasses and bushes (Figure 3). Therefore, the paddy areas that appeared to be in the crop growth phase throughout the time-series images were identified as abandoned due to the absence of paddy planting activities since 2009, while paddy areas depicting planting activities such as land preparation and pre-planting were classified as non-abandoned. This method produced a high accuracy of 93.33% ± 14% and 96.67% ± 0.02% (Tables 3 and 4) in discriminating between abandoned and non-abandoned paddy areas. Figure 8 shows the distribution of these abandoned and non-abandoned paddy areas with the total of 579 ± 82 and 534 ± 0.1 hectares, respectively.
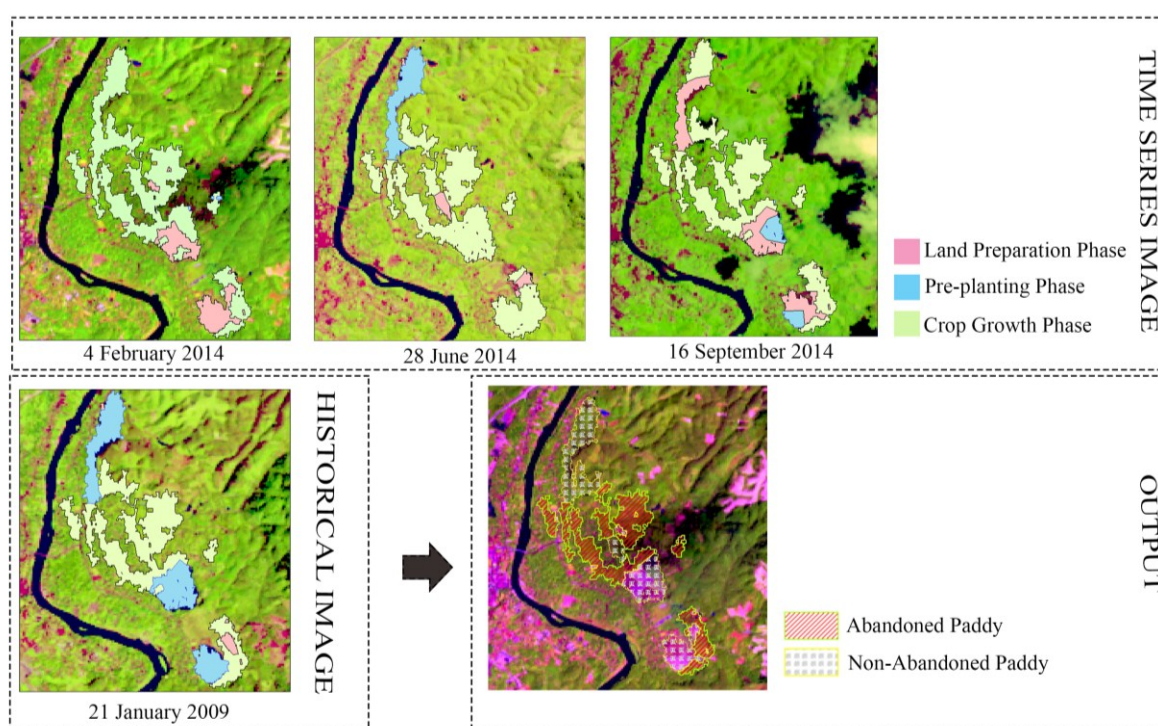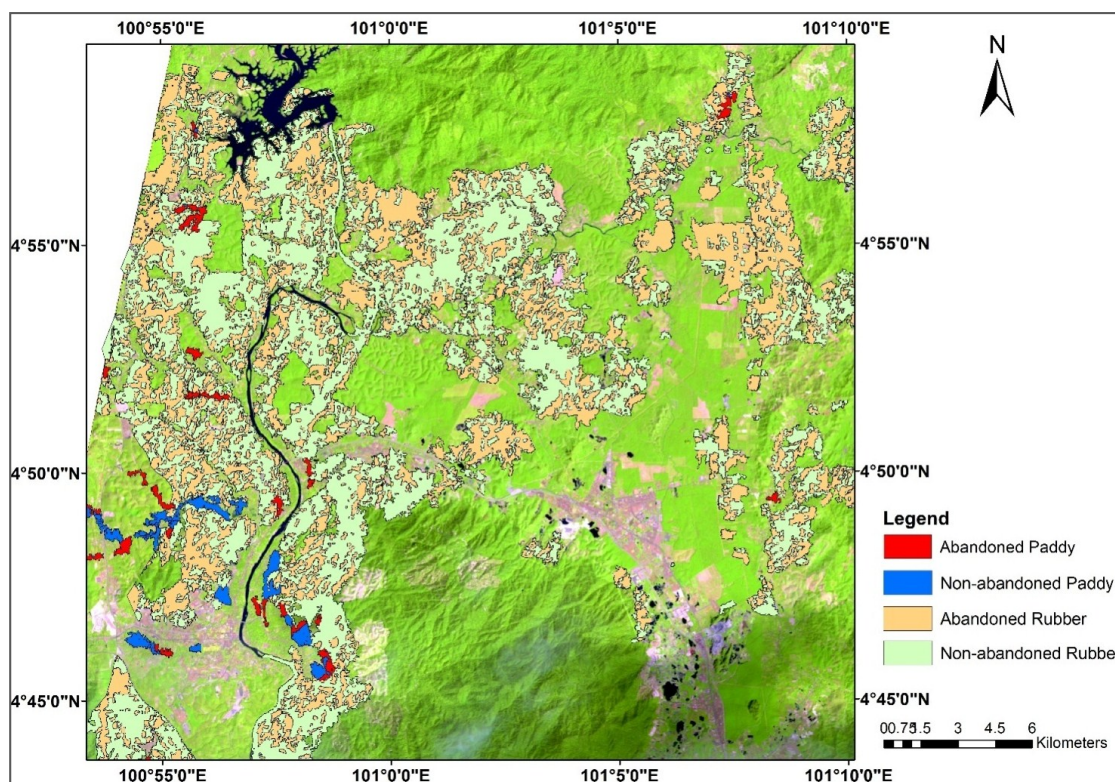

Figure 7. Paddy feature extraction using time-series images and historical image.

Table 3. Accuracy assessment for abandoned and non-abandoned paddy and rubber.

	Abandoned Paddy	Non-abandoned Paddy	Abandoned Rubber	Non-abandoned Rubber	Others	Classification Overall	Producer Accuracy
Abandoned Paddy	28	1	0	0	0	29	96.55%
Non-Abandoned Paddy	0	29	0	0	0	29	100.00%
Abandoned Rubber	0	0	25	0	0	25	100.00%
Non-Abandoned Rubber	0	0	5	26	0	31	83.87%
Others	2			4	0	6	0.00%
Truth Overall	30	30	30	30	0	120	
User Accuracy	93.33%	96.67%	83.33%	86.67%	No Data		

Table 4. Standard Error S(p̂) and Standard Error of Adjusted Area, S(Â).

Class	Map Area (ha)	W*i*	S(p̂)	S(Â)
Abandoned Paddy	579	0.006	0.1408	81.54
Non-Abandoned Paddy	534	0.006	0.0002	0.12
Abandoned Rubber	13,068	0.135	0.0124	162.34
Non-Abandoned Rubber	17,932	0.185	0.1414	2535.11
Others	64,703	0.668		
Total	96,816	1		

Figure 8. Classification Map.

3.2.2. Rubber

Our site visits revealed that abandoned rubber areas were not well organized where the rubber trees were left untapped and the ground was heavily enveloped by bushes (Figure 5). In general, the appearance of abandoned rubber areas was similar to a secondary forest.

Similar to the paddy classification, the usage of historical satellite images is also important to ensure the accuracy of any identified abandoned rubber areas. Since rubber wintering season in the area tends to occur at the beginning of the year, the Landsat image dated as 21 January 2009 was utilized. An 83.33% ± 1% accuracy for the classification of abandoned rubber and an 86.67% ± 14% accuracy for the classification of non-abandoned rubber were achieved in this study, as shown in Tables 3 and 4. Lower accuracy was observed for the non-abandoned rubber primarily due to the presence of evergreen perennial trees such as durian (*Durio* sp.) mixing with the non-abandoned rubber stands in that area. The total areas of these abandoned rubber and non-abandoned rubber were 13,068 ± 162 and 17,932 ± 2535 hectares, respectively, and their distributions are shown in Figure 8.

4. Conclusions

This study shows that the rule-based classification method with the utilization of multi-temporal Landsat images is indeed promising in identifying abandoned paddy and rubber areas where an accuracy of 93.33% ± 14% and 83.33% ± 1%, respectively, were achieved. To differentiate between abandoned and non-abandoned paddy areas, a minimum of three time-series images and an additional historical image are needed in order to meet the definitions of abandonment. As for identifying abandoned rubber areas, the requirement is slightly different. While the feature extraction and classification did not concern the utilization of multi-temporal images, time-series images must be used to confirm the wintering season and, consequently, an image acquired during the wintering time is preferable in order to avoid misclassification. As with the classification of paddy areas, the feature extraction and classification processes still involve the use of an additional historical image.

The total area of abandoned paddy found in this study area is 579 ± 82 hectares, indicating that 52% of paddy area is left uncultivated for almost eight years. Meanwhile, 13,068 ± 162 hectares, or 42% of rubber, is considered as abandoned for the same duration. This study concludes that the use of multi-temporal Landsat images to identify seasonal crop land abandonment, especially paddy and rubber, produces a high level of accuracy.

Acknowledgments

Author Contributions

Noryusdiana Mohamad Yusoff conducted the image processing, collected the ground data, analyzed the data, and wrote the paper. Farrah Melissa Muharam conceived and designed the study, collected the ground data, analyzed the data, and contributed to the revision of the paper.

Conflicts of Interest

The authors declare no conflicts of interest.

References

1. Prishchepov, A.V.; Radeloff, V.C.; Dubinin, M.; Alcantara, C. The effect of Landsat ETM/ETM+ image acquisition dates on the detection of agricultural land abandonment in eastern Europe. *Remote Sens. Environ.* **2012**, *126*, 195–209.
2. Díaz, G.I.; Nahuelhual, L.; Echeverría, C.; Marín, S. Drivers of land abandonment in southern Chile and implications for landscape planning. *Landsc. Urban Plan.* **2011**, *99*, 207–217.
3. Koulouri, M.; Giourga, C. Land abandonment and slope gradient as key factors of soil erosion in mediterranean terraced lands. *Catena* **2007**, *69*, 274–281.

4. Alcantara, C.; Kuemmerle, T.; Baumann, M.; Bragina, E.V.; Griffiths, P.; Hostert, P.; Knorn, J.; Müller, D.; Prishchepov, A.V.; Schierhorn, F.; *et al.* Mapping the extent of abandoned farmland in central and eastern Europe using MODIS time series satellite data. *Environ. Res. Lett.* **2013**, *8*, 035035.

5. Munroe, D.K.; van Berkel, D.B.; Verburg, P.H.; Olson, J.L. Alternative trajectories of land abandonment: Causes, consequences and research challenges. *Curr. Opin. Environ. Sustain.* **2013**, *5*, 471–476.

6. Baumann, M.; Kuemmerle, T.; Elbakidze, M.; Ozdogan, M.; Radeloff, V.C.; Keuler, N.S.; Prishchepov, A.V.; Kruhlov, I.; Hostert, P. Patterns and drivers of post-socialist farmland abandonment in western Ukraine. *Land Use Policy* **2011**, *28*, 552–562.

7. Milenov, P.; Vassilev, V.; Vassileva, A.; Radkov, R.; Samoungi, V.; Dimitrov, Z.; Vichev, N. Monitoring of the risk of farmland abandonment as an efficient tool to assess the environmental and socio-economic impact of the common agriculture policy. *Int. J. Appl. Earth Obs. Geoinf.* **2014**, *32*, 218–227.

8. Gellrich, M.; Baur, P.; Koch, B.; Zimmermann, N.E. Agricultural land abandonment and natural forest re-growth in the Swiss mountains: A spatially explicit economic analysis. *Agric. Ecosyst. Environ.* **2007**, *118*, 93–108.

9. Soukup, T.; Brodsky, L.; Vobora, V. Remote sensing identification and monitoring of abandoned land. Available online: http://www.e-envi2009.org/presentations/S4/Soukup.pdf (accessed on 9 September 2014).

10. Department of Agriculture Official Portal Available online: http://www.doa.gov.my/maklumat-tanah-terbiar (accessed on 12 January 2014).

11. Ponnusamy, R. *Director, Research and Development Division, Felcra Berhad, Kuala Lumpur, Malaysia*; Felcra Plantation Services Sdn.Bhd.: Kuala Lumpur, Malaysia, 2013.

12. Sikor, T.; Müller, D.; Stahl, J. Land fragmentation and cropland abandonment in Albania: Implications for the roles of state and community in post-socialist land consolidation. *World Dev.* **2009**, *37*, 1411–1423.

13. Oetter, D.R.; Cohen, W.B.; Berterretche, M.; Maiersperger, T.K.; Kennedy, R.E. Land cover mapping in an agricultural setting using multiseasonal thematic mapper data. *Remote Sens. Environ.* **2000**, *76*, 139–155.

14. Vieira, M.A.; Formaggio, A.R.; Rennó, C.D.; Atzberger, C.; Aguiar, D.A.; Mello, M.P. Object based image analysis and data mining applied to a remotely sensed Landsat time-series to map sugarcane over large areas. *Remote Sens. Environ.* **2012**, *123*, 553–562.

15. Atkinson, P.M.; Jeganathan, C.; Dash, J.; Atzberger, C. Inter-comparison of four models for smoothing satellite sensor time-series data to estimate vegetation phenology. *Remote Sens. Environ.* **2012**, *123*, 400–417.

16. Dong, J.; Xiao, X.; Chen, B.; Torbick, N.; Jin, C.; Zhang, G.; Biradar, C. Mapping deciduous rubber plantations through integration of PALSAR and multi-temporal Landsat imagery. *Remote Sens. Environ.* **2013**, *134*, 392–402.

17. Dong, J.; Xiao, X.; Sheldon, S.; Biradar, C.; Xie, G. Mapping tropical forests and rubber plantations in complex landscapes by integrating PALSAR and MODIS imagery. *ISPRS J. Photogramm. Remote Sens.* **2012**, *74*, 20–33.

18. Dong, J.; Xiao, X.; Kou, W.; Qin, Y.; Zhang, G.; Li, L.; Jin, C.; Zhou, Y.; Wang, J.; Biradar, C.; *et al.* Tracking the dynamics of paddy rice planting area in 1986–2010 through time series Landsat images and phenology-based algorithms. *Remote Sens. Environ.* **2015**, *160*, 99–113.

19. Stefanski, J.; Chaskovskyy, O.; Waske, B. Mapping and monitoring of land use changes in post-soviet western ukraine using remote sensing data. *Appl. Geogr.* **2014**, *55*, 155–164.

20. Hussain, M.; Chen, D.; Cheng, A.; Wei, H.; Stanley, D. Change detection from remotely sensed images: From pixel-based to object-based approaches. *ISPRS J. Photogramm. Remote Sens.* **2013**, *80*, 91–106.

21. Wang, Z.; Jensen, J.R.; Im, J. An automatic region-based image segmentation algorithm for remote sensing applications. *Environ. Model. Softw.* **2010**, *25*, 1149–1165.

22. Gamanya, R.; de Maeyer, P.; de Dapper, M. Object-oriented change detection for the city of Harare, Zimbabwe. *Expert Syst. Appl.* **2009**, *36*, 571–588.

23. Hall, O.; Hay, G.J. A multiscale object-specific approach to digital change detection. *Int. J. Appl. Earth Obs. Geoinf.* **2003**, *4*, 311–327.

24. Stumpf, A.; Kerle, N. Object-oriented mapping of landslides using random forests. *Remote Sens. Environ.* **2011**, *115*, 2564–2577.

25. Mallinis, G.; Koutsias, N.; Tsakiri-Strati, M.; Karteris, M. Object-based classification using quickbird imagery for delineating forest vegetation polygons in a Mediterranean test site. *ISPRS J. Photogramm. Remote Sens.* **2008**, *63*, 237–250.

26. Abu Bakar, H.A. *Teknologi Perladangan dan Pemprosesan Getah*; Malaysian Rubber Board: Sungai Buloh, Malaysia, 2009.

27. Muhamad Hafiz, A.R. *Geospatial Manager*; Felcra Plantation Services Sdn.Bhd.: Kuala Lumpur, Malaysia, 2014.

28. Guyot, F.B.A.G. Potentials and limits of vegetation indices for LAI and APAR assessment. *Remote Sens. Environ.* **1991**, *35*, 161–173.

29. Leclerc, G.; Hall, C.A.S. *Remote Sensing and Land Use Analysis for Agriculture in Costa Rica*; Academic Press: New York, NJ, USA, 2000.

30. Atzberger, C.; Klisch, A.; Mattiuzzi, M.; Vuolo, F. Phenological metrics derived over the european continent from NDVI3g data and MODIS time series. *Remote Sens.* **2013**, *6*, 257–284.

31. Li, Z.; Fox, J.M. Mapping rubber tree growth in mainland southeast Asia using time-series MODIS 250 m NDVI and statistical data. *Appl. Geogr.* **2012**, *32*, 420–432.

32. De Bie, C.A.J.M.; Khan, M.R.; Smakhtin, V.U.; Venus, V.; Weir, M.J.C.; Smaling, E.M.A. Analysis of multi-temporal SPOT NDVI images for small-scale land-use mapping. *Int. J. Remote Sens.* **2011**, *32*, 6673–6693.

33. USGS. Using the USGS Landsat 8 Product. Available online: http://Landsat.usgs.gov (accessed on 20 January 2015).

34. Chander, G.; Markham, B.L.; Helder, D.L. Summary of current radiometric calibration coefficients for Landsat MSS, TM, ETM+, and EO-1 ALI sensors. *Remote Sens. Environ.* **2009**, *113*, 893–903.

35. Vicenteserrano, S.; Perezcabello, F.; Lasanta, T. Assessment of radiometric correction techniques in analyzing vegetation variability and change using time series of Landsat images. *Remote Sens. Environ.* **2008**, *112*, 3916–3934.

36. Pratt, W.K. *Digital Image Processing*; John Wiley & Sons, Inc: New York, NJ, USA, 1991.

37. ESRI. Band Combinations for Landsat 8. Available online: http://blogs.esri.com/ esri/arcgis/2013/07/24/band-combinations-for-Landsat-8/ (accessed on 20 January 2015).

38. Lian, L.; Chen, J. Research on segmentation scale of multi-resources remote sensing data based on object-oriented. *Procedia Earth Planet. Sci.* **2011**, *2*, 352–357.

39. Gamanya, R.; de Maeyer, P.; de Dapper, M. An automated satellite image classification design using object-oriented segmentation algorithms: A move towards standardization. *Expert Syst. Appl.* **2007**, *32*, 616–624.

40. Karydas, C.G.; Gitas, I.Z. Development of an IKONOS image classification rule-set for multi-scale mapping of mediterranean rural landscapes. *Int. J. Remote Sens.* **2011**, *32*, 9261–9277.

41. Congalton, R.G. A review of assessing the accuracy of classifications of remotely sensed data. *Remote Sens. Environ.* **1991**, *37*, 35–46.

42. Olofsson, P.; Foody, G.M.; Stehman, S.V.; Woodcock, C.E. Making better use of accuracy data in land change studies: Estimating accuracy and area and quantifying uncertainty using stratified estimation. *Remote Sens. Environ.* **2013**, *129*, 122–131.

43. Department, M.M. Monthly Weather Bulletin. Available online: http://www.met.gov.my/ (accessed on 29 May 2015).